DALTON
FULL PAPER

Cyanide-bridged complexes with Sn(II)Mn(I), Sn(II)Mn(II), Sn(IV)Mn(I) and Sn(IV)Mn(II) oxidation states†

Kirsty M. Anderson, Neil G. Connelly, Nicholas J. Goodwin, Gareth R. Lewis, Maria Teresa Moreno, A. Guy Orpen and Andrew J. Wood

School of Chemistry, University of Bristol, Bristol, UK BS8 1TS

Received 19th January 2001, Accepted 15th March 2001
First published as an Advance Article on the web 17th April 2001

The redox-active cyanomanganese carbonyl ligands *trans*- and *cis*-$[Mn(CN)(CO)_2(PR_3)(dppm)]$ (R = OEt or OPh, dppm = $Ph_2PCH_2PPh_2$) and *trans*-$[Mn(CN)(CO)(dppm)_2]$ react with $SnCl_2$ to give $[Cl_2Sn^{II}(\mu\text{-NC})Mn^{I}L_x]$ [L_x = *trans*- and *cis*-$(CO)_2(PR_3)(dppm)$, R = OEt or OPh, **1**–**4**, and *trans*-$(CO)(dppm)_2$ **5**]; complex **5** is oxidised by $[Fe(\eta\text{-}C_5H_5)_2][PF_6]$ to give $[Cl_2Sn^{II}(\mu\text{-NC})Mn^{II}(CO)(dppm)_2][PF_6]$ $\mathbf{5}^+[PF_6]^-$. X-Ray structural studies on the redox related pair **5** and $\mathbf{5}^+$ are consistent with oxidation localised mainly at Mn although the Sn^{II}–NC distance increases from 2.198(3) Å in **5** to 2.303(9) Å in $\mathbf{5}^+$. The dicarbonyl cyanomanganese ligands react with $SnCl_4$ to give trinuclear *trans*-$[Cl_4Sn\{(\mu\text{-NC})MnL_x\}_2]$ [L_x = *trans*- and *cis*-$(CO)_2(PR_3)(dppm)$, R = OEt or OPh, **6**–**9**], X-ray studies on **7** showing octahedral geometry at Sn(IV). The reaction of *cis*-$[Mn(CN)(CO)_2\{P(OEt)_3\}(dppm)]$ with one equivalent each of $SnCl_4$ and PPh_3 and of *trans*-$[Mn(CN)(CO)(dppm)_2]$ with one equivalent each of $SnCl_4$ and $[N(PPh_3)_2]Cl$ gives heterobinuclear $[Cl_4(Ph_3P)Sn^{IV}(\mu\text{-NC})Mn^{I}(CO)_2\{P(OEt)_3\}(dppm)\text{-}cis]$ **10** and $[N(PPh_3)_2][Cl_5Sn^{IV}(\mu\text{-NC})Mn^{I}(CO)(dppm)_2\text{-}trans]$, $[N(PPh_3)_2]^+(\mathbf{11}^-)$, respectively; the latter is oxidised with $[Fe(\eta\text{-}C_5H_5)_2][PF_6]$ to give $[Cl_5Sn^{IV}(\mu\text{-NC})Mn^{II}(CO)(dppm)_2\text{-}trans]$ **11**, completing a series of cyanide-bridged complexes with core oxidation states Sn(II)Mn(I), Sn(II)Mn(II), Sn(IV)Mn(I) and Sn(IV)Mn(II).

Introduction

The redox-active cyanomanganese carbonyls **A**–**C** (Scheme 1)

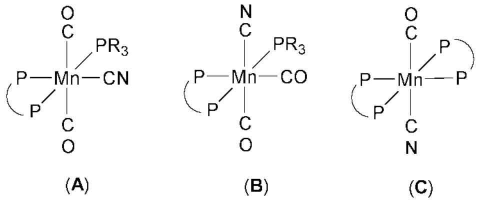

Scheme 1 Cyanomanganese ligands; P–P = dppm, R = OEt or OPh.

can be used as *N*-donor ligands to construct a wide range of bi- and poly-nuclear cyanide-bridged complexes containing M(μ-NC)Mn fragments. The *N*-bound atom can be a redox-active transition metal, *e.g.* in $[(dppm)(CO)_2LMn^{I}(\mu\text{-NC})Mn^{I}(CO)_2L(dppm)]^+$ (dppm = $Ph_2PCH_2PPh_2$; L = PR_3, R = OEt or OPh),[1] $[I(NO)_2Fe^{-I}(\mu\text{-NC})Mn^{I}(CO)(dppm)_2]$,[2] $[Cl_3Fe^{III}(\mu\text{-NC})Mn^{I}(CO)(dppm)_2]$[3] and $[Cl_3Co^{II}(\mu\text{-NC})Mn^{II}(CO)(dppm)_2]$,[4] or a main group element such as Zn,[5] Tl,[6] B[7] or Sb.[8] We now describe the synthesis and characterisation of cyanide-bridged complexes in which the oxidation states of both manganese and a main group element, namely tin, can be systematically varied, *i.e.* in complexes with $Sn^{II}(\mu\text{-NC})Mn^{I}$, $Sn^{II}(\mu\text{-NC})Mn^{II}$, $Sn^{IV}(\mu\text{-NC})Mn^{I}$ and $Sn^{IV}(\mu\text{-NC})Mn^{II}$ cores.

Results and discussion

Bimetallic cyanomanganese complexes of tin(II)

Treatment of the dicarbonyl cyanomanganese ligands *trans*- or *cis*-$[Mn(CN)(CO)_2(PR_3)(dppm)]$ (R = OEt or OPh; **A** and **B** in Scheme 1) in acetone with $SnCl_2$ gave slightly cloudy, yellow reaction mixtures from which $[Cl_2Sn^{II}(\mu\text{-NC})MnL_x]$ [L_x = *trans*-$(CO)_2(PR_3)(dppm)$, R = OEt **1** or OPh **2**; L_x = *cis*-$(CO)_2(PR_3)(dppm)$, R = OEt **3** or OPh **4**] were obtained as yellow powders (Scheme 2). Similarly, the addition of $SnCl_2$ to a suspension of the monocarbonyl cyanomanganese ligand *trans*-$[Mn(CN)(CO)(dppm)_2]$ (**C**, Scheme 1) in thf gave an orange solution from which orange crystals of $[Cl_2Sn^{II}(\mu\text{-NC})Mn^{I}(CO)(dppm)_2]$ **5** were obtained in good yield. Complexes **1**–**5** have been characterised by elemental analysis and IR spectroscopy (Table 1) and, in the case of **5**, by a crystal structure analysis (see below).

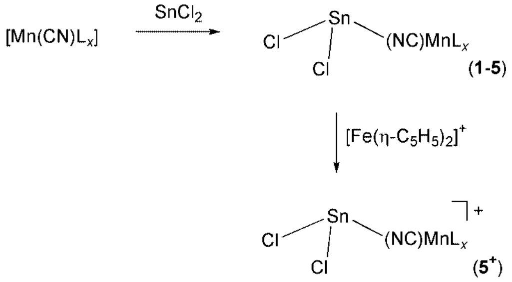

Complex	L_x
1	*trans*-$(CO)_2\{P(OEt)_3\}(dppm)$
2	*trans*-$(CO)_2\{P(OPh)_3\}(dppm)$
4	*cis*-$(CO)_2\{P(OEt)_3\}(dppm)$
4	*cis*-$(CO)_2\{P(OPh)_3\}(dppm)$
5	*trans*-$(CO)(dppm)_2$
5^+	*trans*-$(CO)(dppm)_2$

Scheme 2

The IR spectra of **1**–**5** show a decrease in energy of ν(CN), in the range 9 to 26 cm^{-1}, compared with the mononuclear cyanomanganese precursors, a change which indicates that the

---

† Electronic supplementary information (ESI) available: ν(CO) and $E°'$ data for $[L_nM(\mu\text{-NC})Mn^{I}(CO)(dppm)_2]^z$. See http://www.rsc.org/suppdata/dt/b1/b100721l/

DOI: 10.1039/b100721l

Table 1 Analytical and IR spectroscopic data for $[Cl_nXSn(\mu\text{-}NC)MnL_x]^{z+}$

Complex	L_x	*n*	X	*z*	Colour	Yield (%)	Analysis[a](%) C	H	N	IR[b]/cm^{-1} Cl	ν(CN)	ν(CO)[c]
1	*trans*-$(CO)_2\{P(OEt)_3\}(dppm)$	2	—	0	Yellow	44	47.1 (46.6)	4.4 (4.3)	1.7 (1.6)	—	2062mw	1930 (2006)
2	*trans*-$(CO)_2\{P(OPh)_3\}(dppm)$	2	—	0	Yellow	55	53.9 (54.1)	3.7 (3.7)	1.3 (1.4)	—	2074mw	1943 (2018)
3	*cis*-$(CO)_2\{P(OEt)_3\}(dppm)$	2	—	0	Pale yellow	73	47.1 (46.6)	3.9 (4.3)	1.5 (1.6)	—	2083	1964, 1914m
4	*cis*-$(CO)_2\{P(OPh)_3\}(dppm)$	2	—	0	Pale yellow	78	52.2 (52.5)[d]	3.6 (3.6)	1.5 (1.3)	10.2 (10.0)	2089	1977, 1929m
5	*trans*-$(CO)(dppm)_2$	2	—	0	Orange	66	58.3 (58.5)	4.2 (4.2)	1.3 (1.3)	—	2054mw	1880
$\mathbf{5}^+$	*trans*-$(CO)(dppm)_2$	2	—	1[e]	Dark red	86	50.6 (50.3)[d]	3.4 (3.6)	1.2 (1.1)	8.3 (8.5)	2101	1953
6	*trans*-$(CO)_2\{P(OEt)_3\}(dppm)$	4	$(\mu\text{-}NC)MnL_x$	0	Yellow	79	50.2 (49.9)	4.6 (4.6)	1.8 (1.7)	8.7 (9.0)	2084	1930 (2009vw)
7	*trans*-$(CO)_2\{P(OPh)_3\}(dppm)$	4	$(\mu\text{-}NC)MnL_x$	0	Yellow	60	56.3 (56.5)[d]	3.9 (3.8)	1.5 (1.4)	9.3 (9.0)	2089	1947 (2022vw)
8	*cis*-$(CO)_2\{P(OEt)_3\}(dppm)$	4	$(\mu\text{-}NC)MnL_x$	0	Pale yellow	78	49.1 (49.0)[d]	4.6 (4.5)	1.6 (1.7)	—	2102	1966, 1914ms
9	*cis*-$(CO)_2\{P(OPh)_3\}(dppm)$	4	$(\mu\text{-}NC)MnL_x$	0	Pale yellow	69	56.3 (56.5)[d]	3.9 (3.8)	1.5 (1.4)	—	2104	1978, 1928ms
10	*cis*-$(CO)_2\{P(OEt)_3\}(dppm)$	4	PPh_3	0	Yellow	33	50.3 (50.3)[d]	4.6 (4.3)	1.0 (1.1)	13.9 (14.2)	2099	1967, 1916ms
$\mathbf{11}^-$	*trans*-$(CO)(dppm)_2$	5	—	−1[f]	Orange	73	59.1 (59.5)[g]	3.9 (4.3)	1.5 (1.6)	13.0 (13.8)	2081mw	1874
11	*trans*-$(CO)(dppm)_2$	5	—	0	Bright red	45	52.9 (53.2)	3.7 (3.8)	1.1 (1.2)	15.7 (15.1)	2120	1947

[a] Calculated values in parentheses. [b] In CH_2Cl_2; ν(CN) medium (m) and ν(CO) strong (s) unless stated otherwise; vw = very weak. [c] Weak A-mode given in parentheses. [d] Analysed as a 2 : 1 CH_2Cl_2 solvate. [e] Isolated as $[PF_6]^-$ salt. [f] Isolated as $[N(PPh_3)_2]^+$ salt. [g] Analysed as a 1 : 1 CH_2Cl_2 solvate.

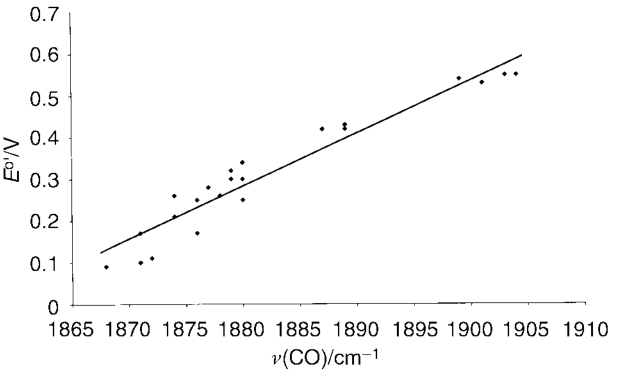

Fig. 1 Plot of $E^{\circ\prime}$ *vs.* ν(CO) for 23 complexes containing the $M(\mu\text{-}NC)Mn^I(CO)(dppm)_2$ fragment.

$Sn^{II}Cl_2$ fragment behaves as a strongly electron-withdrawing group resulting in enhanced dπ–π^* back donation from Mn to CN on cyanide bridge formation; the carbonyl bands of **1**–**5** are at higher energies (by between 10 and 20 cm^{-1}) than those of the cyanomanganese precursors **A**–**C**.

Although complexes **1**–**5** contain redox-active cyanomanganese ligands, most give poorly defined cyclic voltammograms (CVs) at both platinum and gold electrodes in CH_2Cl_2. However, the monocarbonyl complex **5** shows a reversible oxidation wave at a potential (0.30 V) substantially more positive than observed for the mononuclear precursor **C** ($E^{\circ\prime} = 0.07$ V). The large positive shift in $E^{\circ\prime}$, the increase in ν(CO) and the decrease in ν(CN) are all consistent with the *N*-coordinated $Sn^{II}Cl_2$ fragment acting as a strong Lewis acid, reducing the electron density at manganese.

A more quantitative relationship between $E^{\circ\prime}$ and ν(CO) is apparent from the near linear plot (Fig. 1, $R^2 = 0.93$, data collected in ESI)† of potential *vs.* stretching frequency for 23 complexes containing the $(NC)Mn(CO)(dppm)_2$ fragment. Most of these complexes are heterobimetallic, *i.e.* with a $M(\mu\text{-}NC)Mn(CO)(dppm)_2$ core, but also include those in which the terminal nitrogen atom of the cyanide ligand is bound to carbon (*i.e.* isocyanides) or boron. The basis for the linear correlation is not obvious but indicates the relative electron richness of the *N*-bound centres. It is notable, however, that there is a very poor correlation between $E^{\circ\prime}$ and ν(CN) for the same set of complexes.

Chemical oxidation of $[Cl_2Sn^{II}(\mu\text{-}NC)Mn^I(CO)(dppm)_2]$ 5

The CV of $[Cl_2Sn^{II}(\mu\text{-}NC)Mn^I(CO)(dppm)_2]$ **5** suggested that $\mathbf{5}^+$ might be both chemically accessible and stable. Accordingly, **5** was treated with $[Fe(\eta\text{-}C_5H_5)_2][PF_6]$ in CH_2Cl_2 to give a red solution from which $[Cl_2Sn^{II}(\mu\text{-}NC)Mn^{II}(CO)(dppm)_2][PF_6]$ $\mathbf{5}^+[PF_6]^-$ was obtained as dark red crystals. The CV of the salt in CH_2Cl_2 showed a reversible reduction wave at a very similar potential (0.31 V) to that for the oxidation of **5**. The IR spectrum of $\mathbf{5}^+$ (Table 1), showing an increase in both ν(CN) and ν(CO), to 2101 and 1953 cm^{-1} respectively (*cf.* 2054 and 1880 cm^{-1} for **5**), is consistent with one-electron oxidation at manganese, giving a $Sn^{II}(\mu\text{-}NC)Mn^{II}$ core in $\mathbf{5}^+$.

Crystal structures of 5 and $5^+[PF_6]^-$

In order to investigate the structural changes induced by one-electron oxidation, single crystal X-ray diffraction studies were carried out on the redox related pair **5** and $\mathbf{5}^+[PF_6]^-$. Orange crystals of **5** were grown by allowing a concentrated CH_2Cl_2 solution of the complex to diffuse into a 1 : 1 mixture of *n*-hexane : diethyl ether at −10 °C; dark red crystals of $\mathbf{5}^+[PF_6]^-$ were grown by allowing a saturated CH_2Cl_2 solution of the salt to diffuse into *n*-hexane at −10 °C. The structures of one of the two independent molecules of **5** and of $\mathbf{5}^+[PF_6]^-$ are shown in

Table 2 Selected bond lengths (Å) and angles (°) for **5** and **5**$^+$

	5a[a]	**5b**[a]	**5**$^+$
Mn–CN	1.949(3)	1.948(3)	1.977(12)
C–N	1.162(3)	1.168(3)	1.140(14)
Sn–NC	2.204(3)	2.192(3)	2.303(9)
Mn–CO	1.808(3)	1.813(3)	1.845(11)
C–O	1.162(3)	1.158(3)	1.132(13)
Mn–P(ave)	2.275(1)	2.275(1)	2.345(3)
Sn–Cl(ave)	2.463(1)	2.460(1)	2.430(3)
Mn–C–N	177.6(3)	177.8(3)	177.7(9)
C–N–Sn	160.4(2)	164.3(2)	161.7(9)
NC–Mn(1)–CO	175.7(1)	175.6(1)	177.2(5)
P(1)–Mn(1)–P(2)	74.0(1)	73.9(1)	73.0(1)
P(2)–Mn(1)–P(3)	107.9(1)	107.4(1)	105.3(1)
P(3)–Mn(1)–P(4)	74.1(1)	73.9(1)	74.0(1)
P(1)–Mn(1)–P(4)	104.1(1)	104.9(1)	107.9(1)
CN–Sn–Cl(1)	90.0(1)	89.6(1)	91.0(3)
CN–Sn–Cl(2)	91.1(1)	91.5(1)	90.5(2)
Cl(1)–Sn–Cl(2)	96.3(1)	95.5(1)	93.3(1)

[a] **5a** and **5b** are the two independent molecules of **5** in the unit cell.

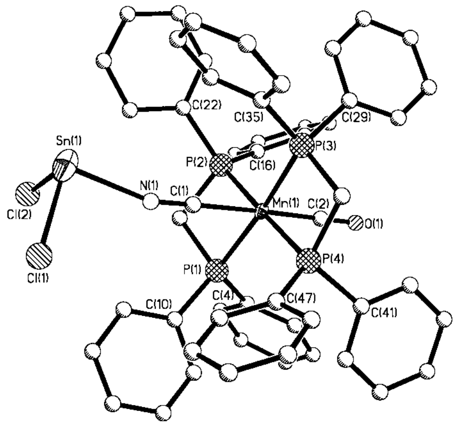

Fig. 2 The structure of one of the two independent molecules of [Cl$_2$Sn^{II}(μ-NC)Mn^I(CO)(dppm)$_2$] **5**. Hydrogen atoms have been omitted for clarity.

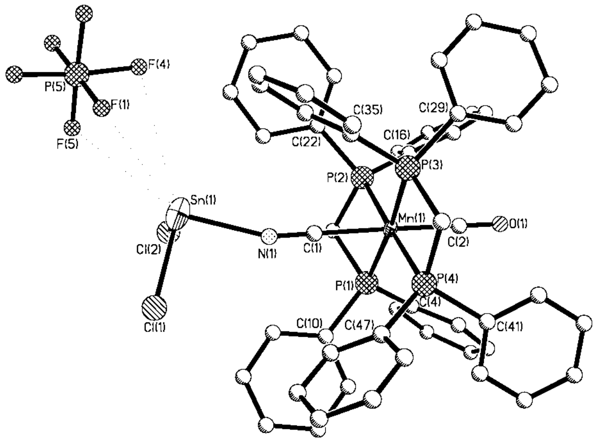

Fig. 3 The molecular structure of [Cl$_2$Sn^{II}(μ-NC)Mn^{II}(CO)(dppm)$_2$][PF$_6$] **5**$^+$[PF$_6$]$^-$. Hydrogen atoms have been omitted for clarity.

Figs. 2 and 3 respectively and selected bond lengths and angles are given in Table 2.

The molecular structure of **5** consists of a slightly distorted octahedral manganese centre coordinated to a dichlorotin(II) moiety. The Mn(μ-CN)Sn unit is significantly non-linear at nitrogen with the C–N–Sn bond angle little more than 160°, as has been observed previously for other complexes containing the *trans*-(dppm)$_2$(CO)Mn(μ-CN)M fragment.[2,4–6,9,10] The tin(II) site is pyramidal (CN–Sn–Cl and Cl–Sn–Cl bond angles in the range 89.6 to 96.3°, *cf.* 109.5° for tetrahedral coordination with a stereochemically active lone pair) as expected for an eight-electron AX$_3$ centre.[11] Similar geometries have been observed in other three-coordinate tin(II) complexes, *e.g.* the bond angles at Sn in the [SnCl$_3$]$^-$ anion of NH$_4$Cl·NH$_4$SnCl$_3$·H$_2$O are 88.1, 88.5 and 88.8°.[12]

The structure of the cation **5**$^+$ shows a significant increase in the average Mn–P bond distance with respect to that of **5**, from 2.275(1) to 2.345(3) Å. Similar differences are observed between the free cyanomanganese complexes *trans*-[Mn(CN)(CO)(dppm)$_2$] and *trans*-[Mn(CN)(CO)(dppm)$_2$]$^+$ [Mn–P(ave) = 2.270(1) and 2.346(5) Å respectively],[13] and the redox-related pair [Cl(OC)$_2$Rh(μ-NC)Mn(CO)(dppm)$_2$-*trans*] and [Cl(OC)$_2$Rh(μ-NC)Mn(CO)(dppm)$_2$-*trans*]$^+$ [Mn–P(ave) = 2.283(1) and 2.352(2) Å respectively].[10] These observations are consistent with the IR spectra noted above, *i.e.* with essentially localised oxidation at manganese to give a heterobinuclear Sn(II)Mn(II) complex. Nevertheless, the Sn–NC distance increases significantly, from 2.204(3) and 2.192(3) Å in **5** to 2.303(9) Å in **5**$^+$, and the average Sn–Cl distance decreases slightly, from 2.463(1) and 2.460(1) Å in **5** to 2.430(3) Å in **5**$^+$. It is not obvious why the Sn–N distance should be so sensitive to the oxidation state of the manganese. (There is no change in the Rh^I–N distance when [Cl(OC)$_2$Rh(μ-NC)Mn^I(CO)(dppm)$_2$-*trans*] is oxidised to [Cl(OC)$_2$Rh(μ-NC)Mn^{II}(CO)(dppm)$_2$-*trans*]$^+$.)

One other aspect of the structures of **5** and **5**$^+$ is of note. In crystals of **5** the two independent molecules of [Cl$_2$Sn^{II}(μ-NC)Mn^I(CO)(dppm)$_2$] are aligned in such a way that the Sn···Sn distance is 3.645(1) Å, less than twice the van der Waals radius of Sn(II) (2 × 2.17 = 4.34 Å, Fig. 4). Two-coordinate tin(II) compounds (stannylenes in particular) are known to form metal–metal bonding interactions[14] through partial donation of the lone pair of one Sn(II) atom into an empty p-orbital of the second. Since all three p-orbitals of the Sn(II) atoms in **5** appear to be involved in Sn–Cl or Sn–N bonding, a Sn···Sn bonding interaction seems unlikely. Nevertheless, the orientation of the SnCl$_2$ moieties in the two molecules of **5** does resemble that of the two SnR$_2$ fragments in the structure of distannenes such as [{(Me$_3$Si)$_2$HC}$_2$SnSn{CH(SiMe$_3$)$_2$}$_2$] {though the Sn–Sn distance of 2.768(1) Å in the latter is much shorter than for **5**}.[15] The crystal structure of **5**$^+$[PF$_6$]$^-$ shows no such Sn···Sn contacts, indicating that oxidation at Mn disrupts the interaction observed in **5**. However, there are three short distances between the tin and fluorine atoms of the [PF$_6$]$^-$ counterion, ranging from 3.33 to 3.76 Å (Fig. 3).

Cyanomanganese complexes of tin(IV)

The dicarbonyls *trans*- or *cis*-[Mn(CN)(CO)$_2$(PR$_3$)(dppm)] (R = OEt or OPh) react with SnCl$_4$ in a 2 : 1 molar ratio in CH$_2$Cl$_2$ to give pale yellow reaction mixtures from which *trans*-[Cl$_4$Sn{(μ-NC)MnL$_x$}$_2$] [L$_x$ = *trans*-(CO)$_2$(PR$_3$)(dppm), R = OEt **6** or OPh **7**; L$_x$ = *cis*-(CO)$_2$(PR$_3$)(dppm), R = OEt **8** or OPh **9**] precipitate as yellow powders on adding *n*-hexane (Scheme 3). Complexes **6**–**9** have been characterised by elemental analysis and IR spectroscopy (Table 1) and, in the case of **7**, by X-ray crystallography. For a given cyanomanganese ligand *ν*(CO) is similar to that of the analogous Sn(II)Mn(I) complexes (*e.g.* compare **1** with **6**, **2** with **7**, *etc.*). However, the increases in *ν*(CN) for **6**–**9** (albeit of less than 10 cm^{-1} compared with the free ligands) contrast with the decreases in *ν*(CN) for **1**–**4**.

Crystals of *trans*-[Cl$_4$Sn{(μ-NC)Mn(CO)$_2$(PR$_3$)(dppm)-*trans*}$_2$]·1.0CH$_2$Cl$_2$ (R = OPh) **7**·1.0CH$_2$Cl$_2$ were grown by allowing a saturated CH$_2$Cl$_2$ solution of the compound to diffuse into *n*-hexane at −10 °C. The molecular structure is shown in Fig. 5 and selected bond lengths and angles are given in Table 3.

Complex **7** has two Mn(I) ligands *trans* disposed about a near

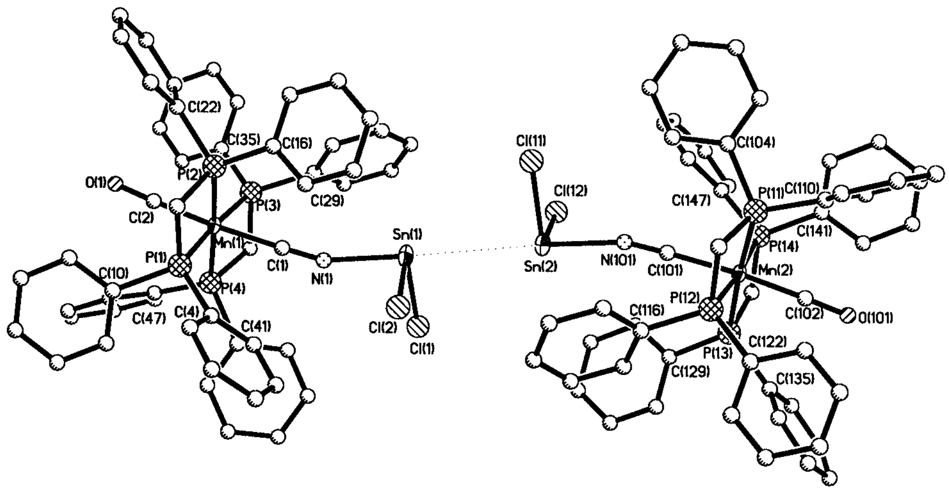

Fig. 4 The alignment in the unit cell of the two independent molecules of $[Cl_2Sn^{II}(\mu\text{-NC})Mn^{I}(CO)(dppm)_2]$ **5**.

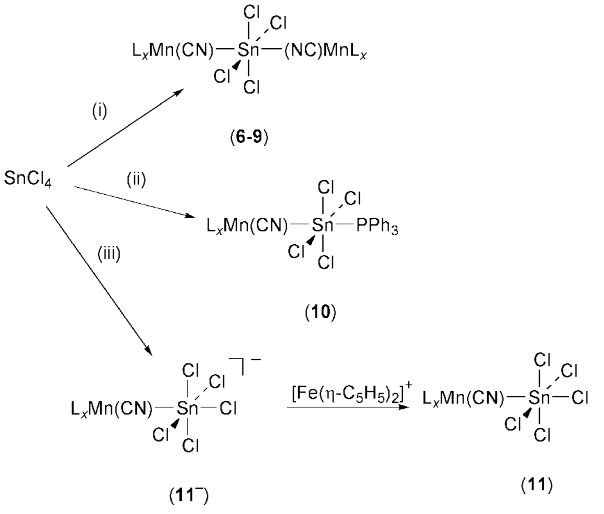

Complex	L_x
6	*trans*-$(CO)_2\{P(OEt)_3\}(dppm)$
7	*trans*-$(CO)_2\{P(OPh)_3\}(dppm)$
8	*cis*-$(CO)_2\{P(OEt)_3\}(dppm)$
9	*cis*-$(CO)_2\{P(OPh)_3\}(dppm)$
10	*cis*-$(CO)_2\{P(OEt)_3\}(dppm)$
11⁻	*trans*-$(CO)(dppm)_2$
11	*trans*-$(CO)(dppm)_2$

Scheme 3 (i) $[Mn(CN)L_x]$, 2 equivs.; (ii) *cis*-$[Mn(CN)(CO)_2\{P(OEt)_3\}(dppm)]$, 1 equiv., PPh_3, 1 equiv.; (iii) *trans*-$[Mn(CN)(CO)(dppm)_2]$, 1 equiv., $[N(PPh_3)_2]Cl$, 1 equiv.

Table 3 Selected bond lengths (Å) and angles (°) for **7**

Mn–CN(ave)	1.928(5)	Mn(1)–C(1)–N(1)	178.1(5)
C–N(ave)	1.160(5)	Mn(2)–C(2)–N(2)	178.0(4)
Sn–NC(ave)	2.144(4)	C(1)–N(1)–Sn	170.6(4)
Mn–CO(ave)	1.842(5)	C(2)–N(2)–Sn	164.6(4)
C–O(ave)	1.145(2)	OC–Mn(1)–CO	170.1(2)
$Mn–P_{dppm}$(ave)	2.292(2)	OC–Mn(2)–CO	175.8(2)
$Mn–P(OR)_3$(ave)	2.196(2)	CN–Sn–Cl	89.0(1)–91.2(1)
Sn–Cl(ave)	2.408(1)	CN–Sn–NC	178.1(1)

regular octahedral Sn(IV) centre, contrasting with the *cis* geometry of the bis(acetonitrile) complex *cis*-$[SnCl_4(NCMe)_2]$.[16] In **7** the CN–Sn–Cl bond angles are in the range 89.0(1) to 91.2(1)° and the average Sn–Cl bond length [2.408(1) Å] is very similar to those in *trans*-$[SnCl_4L_2]$ $\{L = N(Pr^i)=C=NPr^i$, 2.404 Å;[17] $L = N(C_6H_4Cl\text{-}p)=CHPh$, 2.397 Å[18]$\}$ but slightly shorter than in the Sn(II) complexes **5** and **5⁺** (2.46 and 2.43 Å respectively) in accord with the increased effective nuclear charge and smaller ionic radius of Sn(IV). Correspondingly, the average Sn–NC bond length is slightly shorter in **7** [2.144(4) Å] than in **5** [2.198(3) Å], and considerably shorter than in *cis*-$[SnCl_4(NCMe)_2]$ (2.33)[16] and *trans*-$[SnCl_4L_2]$ $\{L = N(Pr^i)=C=NPr^i$, 2.212(3) Å;[17] $L = N(C_6H_4Cl\text{-}p)=CHPh$, 2.267(2) Å[18]$\}$. The latter effect is presumably due, at least in part, to the sp hybridisation of the nitrogen donor atom in **7** (*cf.* sp^2 nitrogens in the imine complexes). The Mn–CN–Sn bridging units in **7** are once again not linear at N, with the two C–N–Sn bond angles 170.6(4) and 164.6(4)°. Presumably due to their steric bulk, the two *trans*-dicarbonyl cyanomanganese ligands are mutually *trans* disposed, the CN–Sn–NC bond angle being 178.1(1)°.

Attempts to synthesise higher nuclearity complexes of the general formula $[Cl_{4-n}Sn\{(\mu\text{-NC})MnL_x\}_{2+n}]^{n+}$ ($n = 1$–4), by reacting **6**–**9** with further equivalents of the appropriate cyanomanganese ligand in the presence of the halide abstraction agent $Tl[PF_6]$, did not give isolable products. *N*-Coordination of six $(NC)Cr(CO)_5$ groups to tin gives the heptanuclear 'star of stars', $[Sn\{(\mu\text{-NC})Cr(CO)_5\}_6]^{2-}$,[19] presumably due to the smaller size of the $Cr(CO)_5$ fragment relative to that of the cyanomanganese ligands.[5] However, a stable bimetallic complex, namely *trans*-$[Cl_4(Ph_3P)Sn(\mu\text{-NC})Mn(CO)_2\{P(OEt)_3\}(dppm)$-*cis*$]$ (**10**), was isolated as a pale yellow solid after addition of one equivalent of PPh_3 to a 1 : 1 mixture of *cis*-$[Mn(CN)(CO)_2\{P(OEt)_3\}(dppm)]$ and $SnCl_4$ in CH_2Cl_2.

A complex analogous to **6**–**9** could not be isolated from the reaction of two equivalents of *trans*-$[Mn(CN)(CO)(dppm)_2]$ with one equivalent of $SnCl_4$ in CH_2Cl_2, but an orange powder slowly precipitated when the reactants were mixed in a 1 : 1 molar ratio. The powder is insoluble even in polar solvents such as thf, acetone and MeCN, but the IR spectrum in Nujol showed a cyanide band at 2066(m) and a carbonyl band at 1897(s) cm^{-1} indicating *N*-coordination of the cyanomanganese ligand. Elemental analysis (C, H and N) was consistent with the molecular formula $[Cl_4Sn\{(\mu\text{-NC})Mn(CO)(dppm)_2\text{-}trans\}]\cdot CH_2Cl_2$; a polymeric structure, with chlorine bridges, would account for the insolubility of the complex.

Stirring a 1 : 1 mixture of *trans*-$[Mn(CN)(CO)(dppm)_2]$ and $SnCl_4$ in CH_2Cl_2 for one minute and then adding one equivalent of $[N(PPh_3)_2]Cl$ gave a pale orange solution from which $[N(PPh_3)_2][Cl_5Sn^{IV}(\mu\text{-NC})Mn^{I}(CO)(dppm)_2\text{-}trans]$ $[N(PPh_3)_2]^+$ (**11⁻**) was isolated on addition of *n*-hexane to the concentrated filtrate.

In common with the CVs of **6**–**10**, that of **11⁻** is ill defined. Nevertheless, the neutral Sn(IV)Mn(II) complex **11** can be prepared by chemical oxidation of **11⁻**. Thus, treatment of the anion with $[Fe(\eta\text{-}C_5H_5)_2][PF_6]$ in CH_2Cl_2 gave a red solution from which $[Cl_5Sn^{IV}(\mu\text{-NC})Mn^{II}(CO)(dppm)_2\text{-}trans]$ **11** was

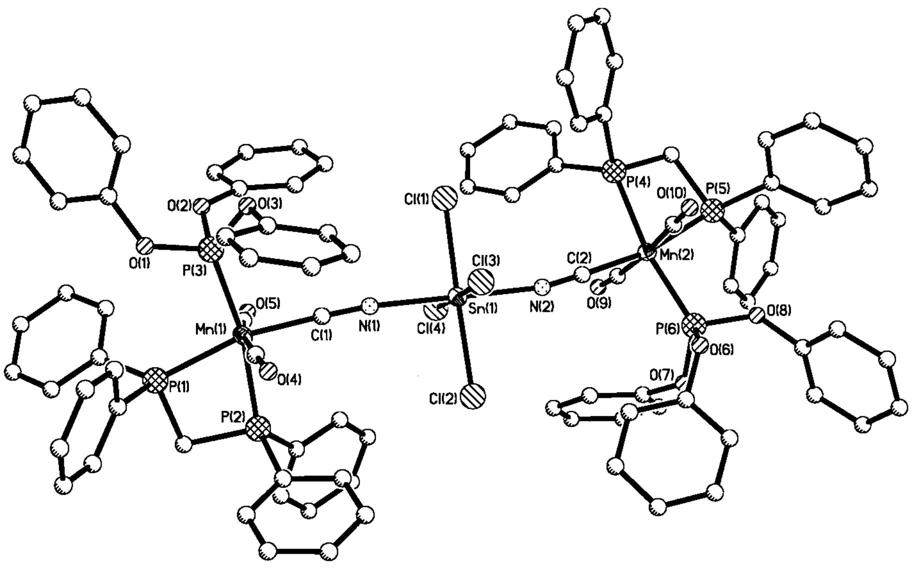

Fig. 5 The molecular structure of *trans*-[$Cl_4Sn\{(\mu\text{-}NC)Mn(CO)_2(PR_3)(dppm)\text{-}trans\}_2$] (R = OPh) **7**. Hydrogen atoms have been omitted for clarity.

obtained as a bright red solid on addition of diethyl ether. The increase in cyanide and carbonyl stretching frequencies (Table 1) on formation of **11** is again consistent with oxidation at manganese, giving a complex with the Sn(IV)Mn(II) core oxidation states.

Conclusion

The cyanomanganese carbonyl ligands *trans*- and *cis*-[$Mn(CN)(CO)_2(PR_3)(dppm)$] (R = OEt or OPh) and *trans*-[$Mn(CN)(CO)(dppm)_2$] react with $SnCl_2$ and $SnCl_4$ to give cyanide-bridged complexes with $Sn^{II}(\mu\text{-}NC)Mn^{I}$ and $Sn^{IV}(\mu\text{-}NC)Mn^{I}$ cores respectively. Chemical oxidation of [$Cl_2Sn^{II}(\mu\text{-}NC)Mn^{I}(CO)(dppm)_2$] **5** and [$N(PPh_3)_2$][$Cl_5Sn^{IV}(\mu\text{-}NC)Mn^{I}(CO)(dppm)_2$-*trans*] [$N(PPh_3)_2$]$^+$**11**$^-$ at the redox-active manganese centres gives **5**$^+$ and **11**, with $Sn^{II}(\mu\text{-}NC)Mn^{II}$ and $Sn^{IV}(\mu\text{-}NC)Mn^{II}$ cores respectively.

X-Ray structural studies on the redox-related pair [$Cl_2Sn^{II}(\mu\text{-}NC)Mn^{I}(CO)(dppm)_2$] **5** and [$Cl_2Sn^{II}(\mu\text{-}NC)Mn^{II}(CO)(dppm)_2$]$^+$ **5**$^+$ are consistent with oxidation at Mn but show significant effects on the Sn–NC distance. Short Sn · · · Sn contacts in **5** are disrupted on oxidation. Complex **7** has octahedral Sn(IV) with *trans* disposed (μ-NC)$Mn^{I}(CO)_2\{P(OPh)_3\}$(dppm)-*trans* units.

Experimental

The preparation, purification and reactions of the complexes described were carried out under an atmosphere of dry dinitrogen using dried, distilled and deoxygenated solvents; reactions were monitored by IR spectroscopy where necessary. The compounds *trans*- and *cis*-[$Mn(CN)(CO)_2(PR_3)(dppm)$] (R = OEt[1] and OPh[20]), *trans*-[$Mn(CN)(CO)(dppm)_2$],[21] [$Fe(\eta\text{-}C_5H_5)_2$][PF_6][22] and [$N(PPh_3)_2$]Cl[23] were prepared by published methods or variations thereof.

IR spectra were recorded on a Nicolet 5ZDX FT spectrometer. Electrochemical studies were carried out using an EG&G model 273A potentiostat (computer-controlled using EG&G model 270 Research Electrochemistry software) in conjunction with a three-electrode cell. For cyclic voltammetry the auxiliary electrode was a platinum wire and the working electrode a platinum or gold disc. The reference was an aqueous saturated calomel electrode (SCE) separated from the test solution by a fine-porosity frit and an agar bridge saturated with KCl. Solutions in CH_2Cl_2 were 0.1×10^{-3} mol dm^{-3} or 5×10^{-4} mol dm^{-3} in the test compound and 0.1 mol dm^{-3} in [NBu_4][PF_6] as the supporting electrolyte. Under the conditions used, $E^{\circ\prime}$ for the one-electron oxidation of [$Fe(\eta\text{-}C_5H_5)_2$], added to the test solutions as an internal calibrant, is 0.47 V. Microanalyses were carried out by the staff of the Microanalytical Service of the School of Chemistry, University of Bristol.

Syntheses

[$Cl_2Sn(\mu\text{-}NC)Mn(CO)_2\{P(OEt)_3\}(dppm)$-*cis*] 3. To a stirred solution of *cis*-[$Mn(CN)(CO)_2\{P(OEt)_3\}(dppm)$] (150 mg, 0.218 mmol) in acetone (20 cm^3) was added $SnCl_2$ (41 mg, 0.216 mmol). After 30 min the reaction mixture was evaporated to dryness *in vacuo*. The residue was extracted into CH_2Cl_2 (20 cm^3) and filtered through Celite before the filtrate was concentrated to *ca.* 10 cm^3 *in vacuo* and a 1 : 1 *n*-hexane : diethyl ether mixture was added (until the mother liquors were almost colourless) to give a pale yellow solid. The product was washed with *n*-hexane (20 cm^3) and dried for 24 h *in vacuo*, yield 140 mg (73%).

The complexes [$Cl_2Sn(\mu\text{-}NC)MnL_x$] [$L_x$ = *trans*-$(CO)_2(PR_3)$(dppm), R = OEt **1** or OPh **2**; L_x = *cis*-$(CO)_2(PR_3)$(dppm), R = OPh **4**] were prepared similarly. Further purification of **4** was achieved by dissolution of the complex in CH_2Cl_2 and addition of *n*-hexane to precipitate a pale yellow product as the 2 : 1 CH_2Cl_2 solvate.

[$Cl_2Sn(\mu\text{-}NC)Mn(CO)(dppm)_2$-*trans*] 5. To a stirred suspension of *trans*-[$Mn(CN)(CO)(dppm)_2$] (250 mg, 0.285 mmol) in thf (40 cm^3) was added $SnCl_2$ (54 mg, 0.285 mmol). After 1 h, the orange solution was evaporated to dryness *in vacuo*. The residue was extracted into CH_2Cl_2 (20 cm^3) and filtered through Celite. The solvent volume was reduced to *ca.* 5 cm^3 and the concentrated solution layered with a 1 : 1 *n*-hexane : diethyl ether mixture and then stored at −10 °C for 6 days to give bright orange crystals, yield 202 mg (66%).

[$Cl_2Sn(\mu\text{-}NC)Mn(CO)(dppm)_2$-*trans*][$PF_6$]·$0.5CH_2Cl_2$ 5$^+$[PF_6]$^-$·$0.5CH_2Cl_2$. To a stirred solution of [$Cl_2Sn(\mu\text{-}NC)Mn(CO)(dppm)_2$-*trans*] (100 mg, 0.094 mmol) in CH_2Cl_2 (20 cm^3) was added [$Fe(\eta\text{-}C_5H_5)_2$][PF_6] (31 mg, 0.094 mmol). After 20 min the red mixture was filtered through Celite. The filtrate was then concentrated to *ca.* 10 cm^3 *in vacuo*, layered with a 1 : 1 *n*-hexane : diethyl ether mixture and stored at −10 °C for two weeks to give dark red crystals, yield 97 mg (86%).

***trans*-[$Cl_4Sn\{(\mu\text{-}NC)Mn(CO)_2(PR_3)(dppm)$-*trans*$\}_2$] (R = OEt 6).** To a stirred solution of *trans*-[$Mn(CN)(CO)_2$-

Table 4 Crystal and refinement data for [$Cl_2Sn(\mu\text{-}NC)Mn(CO)(dppm)_2$] **5**, [$Cl_2Sn(\mu\text{-}NC)Mn(CO)(dppm)_2$][$PF_6$] **5**$^+$[$PF_6$]$^-$ and *trans*-[$Cl_4Sn\{(\mu\text{-}NC)Mn(CO)_2(PR_3)(dppm)$-*trans*$\}_2$]·$CH_2Cl_2$ (R = OPh) **7**·CH_2Cl_2

Compound	**5**	**5**$^+$	**7**·CH_2Cl_2
Empirical formula	$C_{52}H_{44}Cl_2MnNOP_4Sn$	$C_{52}H_{44}Cl_2F_6MnNOP_5Sn$	$C_{93}H_{76}Cl_6Mn_2N_2O_{10}P_6Sn$
M	1067.29	1212.26	2008.65
Crystal system	Triclinic	Orthorhombic	Monoclinic
a/Å	13.344(5)	22.507(3)	11.581(1)
b/Å	18.923(6)	11.769(3)	46.353(6)
c/Å	19.166(4)	19.066(4)	17.523(2)
α/°	91.10(2)	90	90
β/°	93.75(3)	90	94.354(13)
γ/°	96.05(3)	90	90
U/Å^3	4801(3)	5047(2)	9380(2)
T/K	173(2)	173(2)	173(2)
Space group	$P\bar{1}$ (no. 2)	$Pna2_1$ (no. 33)	$P2_1/n$ (no. 14)
Z	4	4	4
μ(Mo-Ka)/mm^{-1}	1.067	1.072	0.860
No. reflections measured	41179	26110	49052
No. unique reflections	16786 (R_{int} = 0.0421)	7908 (R_{int} = 0.0959)	16469 (R_{int} = 0.0836)
*R*1	0.0322	0.0711	0.0574

{$P(OEt)_3$}(dppm)] (200 mg, 0.291 mmol) in CH_2Cl_2 (50 cm^3) was added a 1.57 × 10^{-2} mol dm^{-3} solution of $SnCl_4$ in CH_2Cl_2 (9.3 cm^3, 0.145 mmol). After 30 min the pale yellow mixture was filtered through Celite. The filtrate was then concentrated to *ca.* 20 cm^3, *n*-hexane (40 cm^3) was added, and the solvent volume was further reduced *in vacuo* to give a pale yellow powder which was washed with *n*-hexane (3 × 20 cm^3) and dried, yield 188 mg (79%).

The complexes *trans*-[$Cl_4Sn\{(\mu\text{-}NC)MnL_x\}_2$] [$L_x$ = *trans*-$(CO)_2(PR_3)$(dppm), R = OPh **7**; L_x = *cis*-$(CO)_2(PR_3)$(dppm), R = OEt **8** or OPh **9**] were prepared similarly and isolated as the 2 : 1 CH_2Cl_2 solvates after further purification by dissolution in the minimum volume of CH_2Cl_2, filtration through Celite and addition of *n*-hexane to precipitate pale yellow solids.

***trans*-[$Cl_4(Ph_3P)Sn(\mu\text{-}NC)Mn(CO)_2\{P(OEt)_3\}$(dppm)-*cis*]·0.5$CH_2Cl_2$ 10·0.5CH_2Cl_2.** To a solution of *cis*-[$Mn(CN)(CO)_2\{P(OEt)_3\}$(dppm)] (100 mg, 0.145 mmol) in CH_2Cl_2 (20 cm^3) was added a 1.57 × 10^{-2} mol dm^{-3} solution of $SnCl_4$ in CH_2Cl_2 (9.3 cm^3, 0.145 mmol). The mixture was stirred for 5 min to give a slightly cloudy yellow reaction mixture which, on addition of PPh_3 (38 mg, 0.145 mmol), gave a pale yellow solution. After 1 h the solution was filtered through Celite. The volume of the filtrate was reduced *in vacuo* to less than 10 cm^3 and *n*-hexane was added to precipitate a pale yellow solid which was washed with *n*-hexane (2 × 20 cm^3). The complex was further purified by dissolution in the minimum volume of CH_2Cl_2, filtration and addition of *n*-hexane to the filtrate. The product was dried for 1 h *in vacuo*, yield 60 mg (33%).

[$N(PPh_3)_2$][$Cl_5Sn(\mu\text{-}NC)Mn(CO)(dppm)_2$-*trans*]·$CH_2Cl_2$ [$N(PPh_3)_2$]$^+$(11$^-$)·CH_2Cl_2. To a stirred solution of *trans*-[$Mn(CN)(CO)(dppm)_2$] (150 mg, 0.17 mmol) in CH_2Cl_2 (20 cm^3) was added a 1.57 × 10^{-2} mol dm^{-3} solution of $SnCl_4$ in CH_2Cl_2 (10.9 cm^3, 0.17 mmol) to give a slight lightening in colour of the orange solution. After 1 min, [$N(PPh_3)_2$]Cl (113 mg, 0.17 mmol) was added and the reaction mixture stirred for a further 40 min before filtration through Celite. The filtrate was concentrated to *ca.* 10 cm^3 *in vacuo* and *n*-hexane (40 cm^3) was added to give a pale orange powder which was collected in air and washed with *n*-hexane (3 × 20 cm^3). The complex was further purified by dissolution in CH_2Cl_2, addition of *n*-hexane and reduction of the solvent volume *in vacuo* to precipitate the product. The pale orange solid was collected, washed with *n*-hexane (3 × 20 cm^3), and dried *in vacuo* for 24 h, yield 223 mg (73%).

[$Cl_5Sn(\mu\text{-}NC)Mn(CO)(dppm)_2$-*trans*] 11. To a stirred solution of [$N(PPh_3)_2$][$Cl_5Sn(\mu\text{-}NC)Mn(CO)(dppm)_2$-*trans*] (191 mg, 0.11 mmol) in CH_2Cl_2 (40 cm^3) was added [$Fe(\eta\text{-}C_5H_5)_2$][PF_6] (37 mg, 0.11 mmol). After 10 min the red mixture was filtered through Celite. Reduction of the volume of the filtrate to *ca.* 30 cm^3 followed by addition of diethyl ether (25 cm^3) gave the product as a bright red solid which was washed with diethyl ether (2 × 20 cm^3) and dried *in vacuo* for 1 h, yield 59 mg (45%).

Structure determinations of 5, 5$^+$[PF_6]$^-$ and 7·CH_2Cl_2

Many of the details of the structure analyses of **5**, **5**$^+$[PF_6]$^-$ and **7**·CH_2Cl_2 are presented in Table 4. The structure of **5**$^+$[PF_6]$^-$ contains a disordered [PF_6]$^-$ anion, with two sets of positions for four equatorial fluorines; the major set has an occupancy of 0.57(4). The structure of **7**·CH_2Cl_2 contains dichloromethane disordered over two positions, the major part having an occupancy of 0.599(4).

CCDC reference numbers 160404–160406.

See http://www.rsc.org/suppdata/dt/b1/b100721l/ for crystallographic data in CIF or other electronic format.

Acknowledgements

We thank the EPSRC for Research Studentships (to G. R. L and A. J. W.) and the New Zealand Foundation for Research, Science and Technology for a Postdoctoral Fellowship (to N. J. G.).

References

1 G. A. Carriedo, N. G. Connelly, M. C. Crespo, I. C. Quarmby, V. Riera and G. H. Worth, *J. Chem. Soc.*, *Dalton Trans.*, 1991, 315.
2 F. L. Atkinson, N. C. Brown, N. G. Connelly, A. G. Orpen, A. L. Rieger, P. H. Rieger and G. M. Rosair, *J. Chem. Soc.*, *Dalton Trans.*, 1996, 1959.
3 N. G. Connelly, O. M. Hicks, G. R. Lewis, A. G. Orpen and A. J. Wood, *Chem. Commun.*, 1998, 517.
4 N. G. Connelly, O. M. Hicks, G. R. Lewis, A. G. Orpen and A. J. Wood, *J. Chem. Soc.*, *Dalton Trans.*, 2000, 1637.
5 N. G. Connelly, G. R. Lewis, M. T. Moreno and A. G. Orpen, *J. Chem. Soc.*, *Dalton Trans.*, 1998, 1905.
6 N. G. Connelly, O. M. Hicks, G. R. Lewis, M. T. Moreno and A. G. Orpen, *J. Chem. Soc.*, *Dalton Trans.*, 1998, 1913.
7 D. Bellamy, N. G. Connelly, O. M. Hicks and A. G. Orpen, *J. Chem. Soc.*, *Dalton Trans.*, 1999, 3185.
8 D. Bellamy, N. C. Brown, N. G. Connelly and A. G. Orpen, *J. Chem. Soc.*, *Dalton Trans.*, 1999, 3191.
9 N. C. Brown, G. B. Carpenter, N. G. Connelly, J. G. Crossley, A. Martin, A. G. Orpen, A. L. Rieger, P. H. Rieger and G. H. Worth, *J. Chem. Soc.*, *Dalton Trans.*, 1996, 3977.
10 F. L. Atkinson, A. Christofides, N. G. Connelly, H. J. Lawson, A. C. Loyns, A. G. Orpen, G. M. Rosair and G. H. Worth, *J. Chem. Soc.*, *Dalton Trans.*, 1993, 1441.

11 T. A. Albright, J. K. Burdett and M. H. Whangbo, *Orbital Interactions in Chemistry*, Wiley-Interscience, New York, 1985.

12 P. G. Harrison, B. J. Haylett and T. J. King, *Inorg. Chim. Acta*, 1983, **75**, 265.

13 G. A. Carriedo, N. G. Connelly, E. Perez-Carreño, A. G. Orpen, A. L. Rieger, P. H. Rieger, V. Riera and G. M. Rosair, *J. Chem. Soc., Dalton Trans.*, 1993, 3103.

14 K. M. Baines and W. G. Stibbs, *Adv. Organomet. Chem.*, 1996, **39**, 275.

15 P. J. Davidson, D. H. Harris and M. F. Lappert, *J. Chem. Soc., Dalton Trans.*, 1976, 2268; D. E. Goldberg, P. B. Hitchcock, M. F. Lappert, K. M. Thomas, A. J. Thorne, T. Fjeldberg, A. Haaland and B. E. R. Schilling, *J. Chem. Soc., Dalton Trans.*, 1986, 2387.

16 M. Webster and H. E. Blayden, *J. Chem. Soc. A*, 1969, 2443.

17 H.-D. Hausen, W. Schwarz, G. Rajca and J. Weidlein, *Z. Naturforsch., Teil B*, 1986, **41**, 1223.

18 K. G. Rasmussen, K. Juhl, R. G. Hazell and K. A. Jorgensen, *J. Chem. Soc., Perkin Trans. 2*, 1998, 1347.

19 M. Fritz, D. Rieger, E. Bär, G. Beck, J. Fuchs, G. Holzmann and W. P. Fehlhammer, *Inorg. Chim. Acta*, 1992, **200**, 513.

20 G. A. Carriedo, M. C. Crespo, V. Riera, M. G. Sanchez, M. L. Valin, D. Moreiras and X. Solans, *J. Organomet. Chem.*, 1986, **302**, 47.

21 A. Christofides, N. G. Connelly, H. J. Lawson, A. C. Loyns, A. G. Orpen, M. O. Simmonds and G. H. Worth, *J. Chem. Soc., Dalton Trans.*, 1991, 1595.

22 N. G. Connelly and W. E. Geiger, *Chem. Rev.*, 1996, **96**, 877.

23 J. K. Ruff and W. J. Schlientz, *Inorg. Synth.*, 1974, **15**, 84.